Diffusion of salt through electrified porous carbon

studied with the colloidal charge sensor

Jeroen Huijben

Supervisor: dr. Ben Erné

Bachelor's thesis in Chemistry

Van 't Hoff Laboratory for Physical and Colloid Chemistry

Utrecht University

July 2017

Abstract

In this thesis the diffusion of salt through porous carbon is studied. In particular, we use the colloidal charge sensor setup [1, 2] to determine the diffusion rate of salt through an externally charged porous carbon membrane. We succeeded in performing these measurements, but we had to use a few workarounds for practical problems. Salt transport across the membrane appeared to occur mainly via wide pores in which ions are hardly affected by changes in surface charge.

Acknowledgements

I would like to thank a number of people: Ben Erné for his (patient) supervision over the last year; Albert Philipse for being the second reviewer of this thesis; and everyone at FCC now and last year, for a nice time while I was there. I would also like to thank friends and family, in particular Iris van Dalen, for motivating me to finish this thesis.

Contents

Chapter 1

Introduction

Transport of salt through a porous network is important in many applications. A major example is dialysis. A solution of macromolecules and a salt is inside a bag of dialysis membrane. This bag sits inside a solution of another salt. The dialysis membrane is semi-permeable: the pores are large enough for the salt to pass through, but not for the macromolecule. The salt concentrations equilibrate over the membrane, and in this way the salt inside the bag is exchanged for the salt on the outside.

Another application is a novel sensor that measures the charge-to-mass ratio of colloids and macromolecules [1, 2]. A small compartment filled with a saline solution, is in contact with a large compartment filled with the same saline solution. In between the two membranes is a semi-permeable dialysis membrane. If a charged colloid or macromolecule with mobile counter-ions is dissolved in the large compartment, there will be an excess of salt in the large compartment, and this causes diffusion of salt into the small compartment. By measuring the concentration increase inside of the small compartment, the charge-to-mass ratio of the colloid or macromolecule can be determined. In this application we see again an important step is diffusion of ions through a porous network.

From another angle, we also see the transport of ions through porous networks in blue energy. Let us consider the method of capacitive mixing for this [3]. This is a method for extracting energy from the mixing of salt and fresh water. It uses a compartment where two carbon electrodes are mounted. These carbon electrodes have a very porous structure. Typically the electrodes have a specific surface area of $1000\,\mathrm{m}^2/\mathrm{g}$, achieved by many pores of only 1 nm in diameter. First salt water is brought into the compartment, and a potential difference is applied between the two electrodes. This charges the carbon electrodes, and charge neutrality is preserved by negative ions moving into the positive electrode, and vice versa. The counter-ions form an electric double layer at the electrode surface, which entirely shields the charge on the electrodes. When the ions are stored inside of the electrodes, the circuit is opened and fresh water is brought into the compartment. The double layers at the electrode surface still have the same charge density, but at a lower ionic strength the potential over this double layer increases. Therefore the potential difference between the two electrodes increases. When the circuit is closed, the ions in the double layer are again dissolved and the charge on the electrodes flow back at a higher

potential than during the charging. Therefore this system performs positive net electrical work, by mixing salt and fresh water.

In this last application, we see the transport of ions through a porous network, but the network is charged in this case. We imagine that the charge does not only attract the ions, but also influences their transport. This is the issue that we address in this thesis. We aim to characterise the diffusion rate of salt through a porous carbon membrane and to measure the effect of charging the carbon membrane. We mainly focus on the practical aspects of these questions and try to decide if it is possible to do these measurements using the colloidal charge sensor to measure salt transport across the membrane.

1.1 Research questions

Based on these considerations, we pose the following three research questions:

1. Can we measure the diffusion rate of salt through a porous carbon membrane?
2. Can we measure this diffusion rate when the membrane is being charged by an external power source?
3. Can we see the influence of charge on the diffusion rate?

Chapter 2

Theory

2.1 Electric double layer structure

The porous carbon membrane is charged by applying an external potential. Here we describe the expected charge density as function of this potential.

Our porous carbon electrodes have the following structure: there are large macropores in the carbon membrane with diameter of the order 1 µm. On the surface of these macropores, there are micropores of diameter of the order 2 nm.

When a voltage is applied to the carbon material, charge will accumulate on the carbon matrix. To preserve charge neutrality, counter-ions will move towards the surface, while ions of the same sign are expelled from the surface. This creates an electrical double layer with charge inside the carbon compensated by ions at and in the vicinity of the surface.

To describe the resulting charge density, different models have been devised over time. One is the Gouy-Chapman model with adaptations by Stern [4]. The Gouy-Chapman model describes the equilibrium between the electrostatic forces and the diffusion of the ions. Under the assumption that the charged surface is a flat, infinite sheet, this model gives a potential that is exponentially decaying with the distance to the surface. The predicted double layer is called the Gouy-Chapman diffuse layer. In particular we find the following relation between the electric charge per unit area in the double layer (denoted σ) and the electric potential over the double layer (denoted by Ψ):

$$\sigma = -\sqrt{8\epsilon_0\epsilon_m CRT}\sinh\frac{F\Psi}{2RT}.$$

Here ϵ_0 is the permittivity of vaccum, ϵ_m the relative permittivity of the medium, C is the ion concentration, R is the universal gas constant, T the temperature and F the Faraday constant. This shows that the charge on the carbon membrane can be tuned, by tuning the potential of the membrane.

With this formula we can also compute the differential capacitance of the electric double

layer. This is given by

$$\frac{d\sigma}{d\Psi} = c_1 \cosh \frac{F\Psi}{2RT}.$$

Here c_1 is a constant which does not depend on Ψ (the exact value of c_1 is $-F\sqrt{\frac{2\epsilon_0\epsilon_m C}{RT}}$). We see that the differential capacitance has an extremum at $\Psi = 0$, which corresponds to $\sigma = 0$.

However, this model fails for highly charged double layers, as it predicts an impossible concentration of counter-ions near the surface. Due to the finite size of the ions, they cannot be arbitrarily close to the surface, and therefore the concentration very near to the surface is zero. To remedy this, the so-called Stern layer is introduced. This consists of counter-ions which are adhered to the surface, compensating the low concentration directly near the surface. Between the surface and this Stern layer, the potential decreases linearly, while the system after the Stern layer can again be described as a Gouy-Chapman double layer.

The Stern layer and the Gouy-Chapman diffuse layer together store the the necessary counter-charge to the carbon matrix, and they shield the electric field of the carbon away from the surface. Therefore the typical width of the double layer is important in determining the properties of the carbon membrane. If the double layer covers an entire pore, there will be a potential barrier for salt to enter the pore.

In aqueous saline solutions and for a flat charged surface, the Debye length is typical for the double layer width. This still holds for double layers in pores, see e.g. [5]. In the concentration range around 10 mmol, the Debye length is in the order of a few nm, which is about the size of the micropores [6].

2.2 Ion diffusion through charged pores

The rate of ion diffusion will depend on the electric potential in the membrane. If the membrane is charged, this potential will be largely dependent on the electrical potential caused by the charge of the membrane. In the previous section we have seen that the electrical potential inside the membrane is mainly determined by the Gouy-Chapman double layers, and the thickness of these double layers is in the order of the Debye length.

If the diameter of a pore is much larger than the Debye length, which is the case for the macropores in our carbon membrane, the electric potential in the center of the pore is the same as outside of the membrane. Therefore the charge on the carbon membrane will have very little influence on the diffusion of ions through the membrane.

On the other limit, the Debye length is much larger than the pores. The electric potential in the pore is then much higher than outside of the membrane, so we expect that the co-ions are completely blocked from the pores. Because diffusion of neutral salt requires both types of ion to diffuse through the membrane, diffusion would be negligible.

In between, we have the situation where the pore has the same size as the Debye length. This occurs for the micropores in our carbon membrane. Then the electric potential inside of the pores will differ from the potential outside of the membrane. This electrical potential will act as a potential well for one type of ion, while it is a potential barrier for the other type. Because of charge neutrality, both ions have to move through the pore. So the rate of diffusion depends on the balance between the repulsion of co-ions, and attraction of counter-ions. In [7], we see that in this range the diffusion of salt can already decrease significantly.

Chapter 3

Experimental methods

In this chapter we first discuss the method used to charge the carbon membrane. Then we describe how the salt diffusion rate is determined, and next we describe how the diffusion rate is determined while the carbon membrane is kept at an applied potential.

3.1 Charge sensor setup

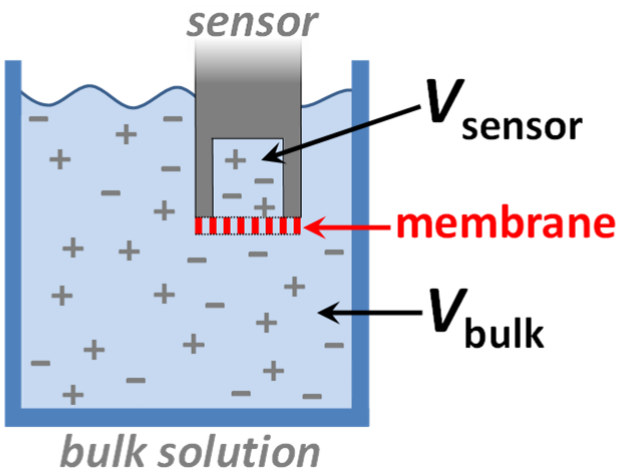

Figure 3.1: Schematic view of charge sensor setup (reproduced from [2]). The setup is filled with an aqueous NaCl solution.

The measurements are performed using the setup of the charge sensor, developed at the FCC lab [1, 2]. A schematic view of this setup is shown in figure 3.1. The bulk compartment contains a NaCl solution, which is in contact with the solution in the sensor compartment through a porous membrane.

The sensor compartment has a volume of about 2 µL, and the bulk compartment a volume of about 20 mL. Furthermore there is a glass wall around the bulk compartment with a separate compartment. This is filled with water from a thermostat, thus keeping the

temperature of the vessel constant at 25 °C. The top is completely sealed by the sensor, and therefore there are two arms extending into the bulk compartment. These arms can be used to make changes to the bulk solution, and to introduce extra electrodes.

3.2 Electrometers

To do electrical experiments and measurements, a PAR (Princeton Applied Research) 8-channel potentiostat is used, with 8 frequency analyzers of model PMC 1000. They are used with VersaSTAT software.

3.3 Electric charging of porous carbon membrane

To charge the porous carbon membrane, a three-electrode setup is used. In this setup, the carbon membrane is used as working electrode (WE), and an 0.5mm platinum wire is used as counter electrode (CE). An Ag/AgCl electrode (model Radiometer Analytical REF200) is used as reference electrode (RE). This consists of a silver wire coated in silver chloride, and immersed in a saturated potassium chloride solution. This gives the silver electrode a fixed potential. The electrode solution is in contact with the compartment via a porous plug.

In practical terms the working electrode and the counter electrode are brought into the bulk compartment through the two arms, see figure 3.3. To make the carbon membrane into the working electrode, an electrical contact is made by pressing a pencil lead into the membrane from the top. The other side of the pencil lead is glued to a copper wire with conducting glue. See figure 3.2.

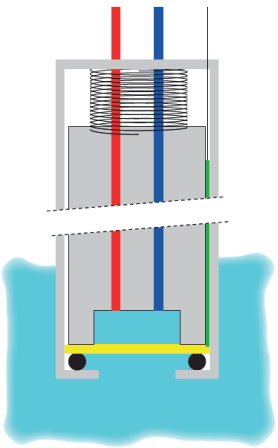

Figure 3.2: Schematic view of sensor probe (reproduced from [8]). The yellow membrane represents the porous carbon membrane, the green line a pencil lead used to make the electrical contact. With conducting glue, the lead is glued to a copper wire (in black).

In this setup, a potential difference is imposed between the working electrode and the counter electrode. This induces a charge build-up in the carbon membrane. To maintain charge neutrality, one type of ion moves toward the membrane, while the other type of ions moves away. To close the circuit, a redox reaction takes place at the platinum surface. Hence the potential difference will charge the carbon membrane. The WE-CE potential difference is continually tuned, such that the WE-RE potential difference is at the desired value. We use the reference electrode for this, to exclude electrical effects on the platinum surface from the measurement.

When the potential of the membrane is changed, we measure the current from membrane to CE, to determine the charge accumulated on the membrane.

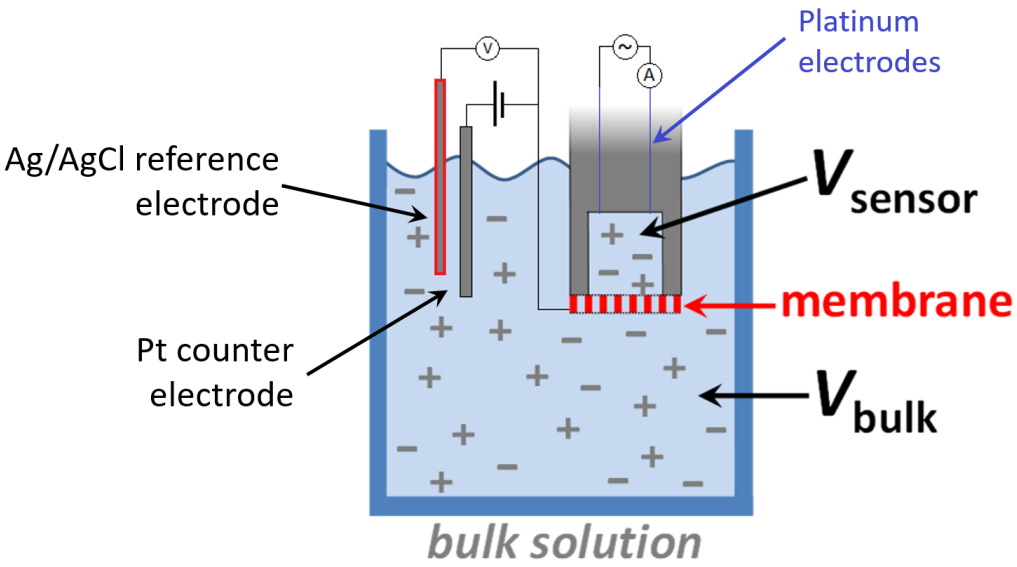

Figure 3.3: Schematic view of charge sensor setup (reproduced from [2]). The Ag/AgCl reference electrode and Pt counter electrode are used to charge the porous carbon membrane. The platinum electrodes in the sensor compartment are used to determine the salt concentration.

3.4 Determining diffusion rate through porous carbon membrane

The approach to determine the diffusion rate through the porous carbon membrane is as follows. We put a 1 mM NaCl solution in the bulk and sensor compartment. Under continuous stirring, we add with a syringe approximately 0.2 mL of a 1 M NaCl solution to the bulk compartment, via one of the arms. This increases the salt concentration in the bulk compartment by about 10 mM. Then we measure the concentration in the top of the sensor compartment over time. This gives the diffusion rate of salt from the bulk compartment through the membrane, and from the membrane to the top of the sensor compartment.

3.5 Measuring salt concentration in sensor compartment

The resistivity of the salt solution in the sensor compartment is inversely proportional to the concentration. Hence the concentration can be determined by measuring the resistance between two fixed points inside the sensor solution. In the setup two platinum tips are placed on the top of the sensor compartment, and we determine the resistance between the two. Because of capacitive effects of the double layer formed at the platinum surface, the resistance cannot be determined by a direct current measurement, and therefore electronic impedance spectroscopy (EIS) is used.

Impedance, denoted by Z, is a complex-valued quantity and is a generalisation of resistance to alternating current circuits. If an alternating potential is applied over an electrical circuit, say described by $V_0 \sin(\omega t + \phi_V)$, this results in an alternating current. This current must have the same frequency as the potential, but there may be a phase change between the waves. If we assume V_0 to be small enough, the response current will be approximately sinusoidal, and it can be described by $I_0 \sin(\omega t + \phi_I)$. The impedance of the electrical circuit is then given by $Z = \frac{V_0}{I_0} e^{i(\phi_V - \phi_I)}$. This has absolute value V_0/I_0, which is similar to the resistance. However, the argument of Z (the angle with the positive real axis) is $\phi_V - \phi_I$ and this describes the phase difference between the potential and the current. Because impedance is a complex valued quantity, its values should be represented in a complex plane.

The quantity ω is called the angular frequency, and has units $\mathrm{rad\,s^{-1}}$. It is related to the normal frequency f by $\omega = (2\pi\,\mathrm{rad}) \cdot f$. In general the impedance Z will depend on this angular frequency. For example, we can compute the impedance of a few standard elements in an electrical circuit. A resistor with resistance R simply has impedance $Z = R$. A capacitor (e.g. two large metal sheets separated by a thin insulating layer) with capacitance C, has impedance $\frac{1}{i\omega C}$.

Impedance shares certain properties with resistance. For example, two elements with impedances Z_1 and Z_2 that are connected in series have a total impedance of $Z_1 + Z_2$. If they are connected in parallel, the total impedance is $\frac{1}{1/Z_1 + 1/Z_2}$.

In electrical impedance spectroscopy, we measure the impedance of the electrical system at a range of varying frequencies. To obtain the resistance from the EIS, we have to model the entire system with an electrical circuit. The solution is modelled as a resistance and capacitor connected in parallel. The electrical double layer at the platinum surface is modelled by a constant phase element (CPE).

A CPE generalizes the concepts of resistance and capacitor, and has behaviour which is in between these two elements. The impedance of this element is given by $\frac{1}{q_0 (i\omega)^n} = \frac{e^{-n\pi i/2}}{q_0 \omega^n}$, where n is a number between 0 and 1, and q_0 gives (up to units) the absolute value of the impedance at $\omega = 1\,\mathrm{rad\,s^{-1}}$. By taking $n = 0$, we get impedance $1/q_0$ which is the impedance of a resistor if we take $q_0 = 1/R$. By taking $n = 1$, we get impedance $\frac{1}{iq_0\omega}$ which is the impedance of a capacitor if we take $q_0 = C$. So we see that a CPE indeed generalises both a resistor and a capacitor. Formally the unit of q_0 will be $\Omega^{-1}\mathrm{s^n rad^{-n}}$,

which has no good physical meaning when n is not an integer. Therefore we will only give the numerical value of q_0, and keep in mind that its unit should be $\Omega^{-1}\mathrm{s}^{\mathrm{n}}\mathrm{rad}^{-\mathrm{n}}$.

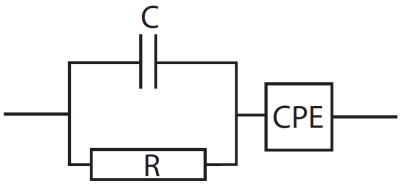

Figure 3.4: Circuit used to model the NaCl solution between the platinum tips.

The model circuit is shown in figure 3.4. Now we compute the impedance of this circuit. For this we let ω be the angular frequency of the alternating potential. The resistance and the capacitor have respective impedances R and $\frac{1}{i\omega C}$, so their combined capacitance is $\frac{1}{1/R+i\omega C}$. The CPE has impedance $\frac{e^{-n\pi i/2}}{q_0\omega^n}$, so together this gives

$$Z = \frac{1}{1/R + i\omega C} + \frac{e^{-n\pi i/2}}{q_0\omega^n}.$$

Fitting this formula to the measured data, we find the values of the desired parameters and in particular we find the resistance.

3.6 Diffusion through electrified carbon membranes

To answer the second question, we simultaneously charge the carbon membrane, and determine the diffusion rate through the membrane by measuring the concentration in the sensor compartment. By varying the potential of the carbon membrane, we also vary the charge on the membrane. Repeating the same procedures, we determine the diffusion speed of salt through the porous carbon membrane, at different membrane charges.

Chapter 4

Results and discussion

In this section we present and discuss the results of the measurements described in the *Experimental methods* chapter. Some of the figures in this chapter are quite large, and have therefore been moved to the end of the chapter.

4.1 Charging carbon

The potential difference between the carbon membrane and the reference electrode was measured to be 330 mV. The potential of the membrane was instantaneously increased with steps of 100 mV, up to 630 mV. The measured currents are shown in figure 4.1. The measurements were performed in a 1 mM NaCl solution, but this increased during the experiment to at least 40 mM (see sections 4.3 and 4.5).

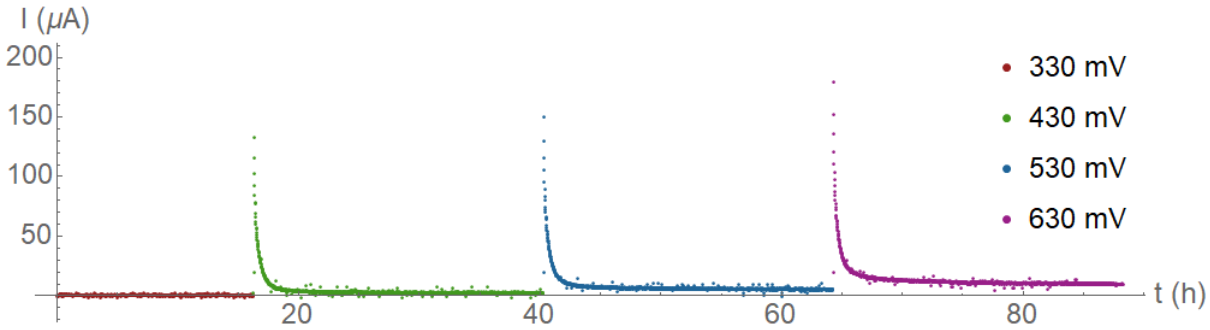

Figure 4.1: Current while charging the porous carbon membrane in aqueous NaCl solution at various potentials vs Ag/AgCl. The NaCl concentration ranged from 1 mM to at least 40 mM.

As expected, we see a fast decay of the current. If there was only a current charging the membrane, we expect the current to converge to 0 A. However, we see that a constant non-zero current is reached in the last two cases. This indicated that not only charging

of the membrane takes place, but that redox reactions also take place at the membrane surface.

To determine the current used for charging the membrane, we assume that the redox current is linearly dependent on time. We estimate this linear dependency from the last 12 hours of the current curve. Then we subtract this current from the entire curve, and numerically integrate to find the charge on the carbon membrane.

Another problem lies in the settings used by the measurement apparatus. The apparatus automatically switched between various measuring ranges for measuring the current. The relevant ranges are: up to 2 µA, up to 20 µA, and up to 200 µA. To choose a range, it considers the last measured point and chooses the lowest range containing this value. This gives a problem at the moment when the potential is increased. Just before the increase, the current is low and the range up to 20 µA is used. But after the potential increase, the current will be much higher than 20 µA. The apparatus then only reports that the value is larger than 20 µA and we miss the first data point. Because this is a high value, this induces an error in the charge determination.

We corrected for the redox current, but we could not compensate for the missing value at the start. The results of the charge determination are shown in table 4.2.

V vs Ag/AgCl (mV)	ΔQ (C)
330	0.00
430	0.17
530	0.36
630	0.61

Figure 4.2: Charge difference on the carbon, relative to the point $V_{WE-RE} = 330\,\mathrm{mV}$.

We quickly check whether these values correspond with the Gouy-Chapman theory. When the potential over the electric double layer at the carbon surface is not too large, we can use the approximation $\sinh x \approx x$ to get $\sigma \approx -\Psi F\sqrt{\frac{2\epsilon_0\epsilon_m C}{RT}}$. When plugging in the values $\epsilon_m = 80$ (relative permittivity of water, [9]), $C = 10\,\mathrm{mM} = 10\,\mathrm{mol/m^3}$ and $\Psi = 100\,\mathrm{mV}$, we get $\sigma \approx 0.023\,\mathrm{C/m^2}$. The properties of the porous carbon membrane have been determined before [10, 11], in particular it has a thickness of 0.5 mm, a mass density of $0.58\,\mathrm{g\,mL^{-1}}$, and a specific surface of $1330\,\mathrm{m^2/g}$. The membrane is a disk of about 1.5 cm in diameter, which gives a specific surface of $68\,\mathrm{m^2}$. Hence the potential increase from 330 mV to 430 mV gives a change in surface charge density of of $0.0025\,\mathrm{C/m^2}$. The difference with the prediction from theory is a factor 10, but we know that assumption from the theory (flat sheet of charged surface) is not true. Therefore we can only say that the measured surface charge is in the same order as predicted by the theory.

We see that we can find out how much the charge on the membrane changes as the potential changes. However, in this way we cannot determine the actual charge on the membrane, as we don't know when the membrane is uncharged. At open circuit potential, the membrane is not necessarily uncharged, because the membrane may have charged surface groups [12]. As the Gouy-Chapman theory shows, the point of zero charge can

be found by determining the largest slope in the $\Delta Q, V$-diagram [13]. With the measurements we have performed, we have too few data points to make a meaningful estimate of the slope in the diagram. Therefore we cannot determine the point of zero charge.

4.2 Electrical impedance spectrometry

We first performed EIS measurements on a solution of 0.1 M NaCl solution in the sensor compartment, with frequencies from 1 Hz to 100 kHz. This showed some limitations of the apparatus. First of all, we plotted the phase of the impedance against the measuring frequency, this is shown in figure 4.3 for 50 measurements. We clearly see distinct lines of distinct measuring ranges used by the apparatus. The raw data shows that between these ranges the apparatus has a 1 second pause, which also indicates that it switches the measuring range. Because these ranges are not well calibrated with respect to each other, we should pay attention to this in subsequent measurements.

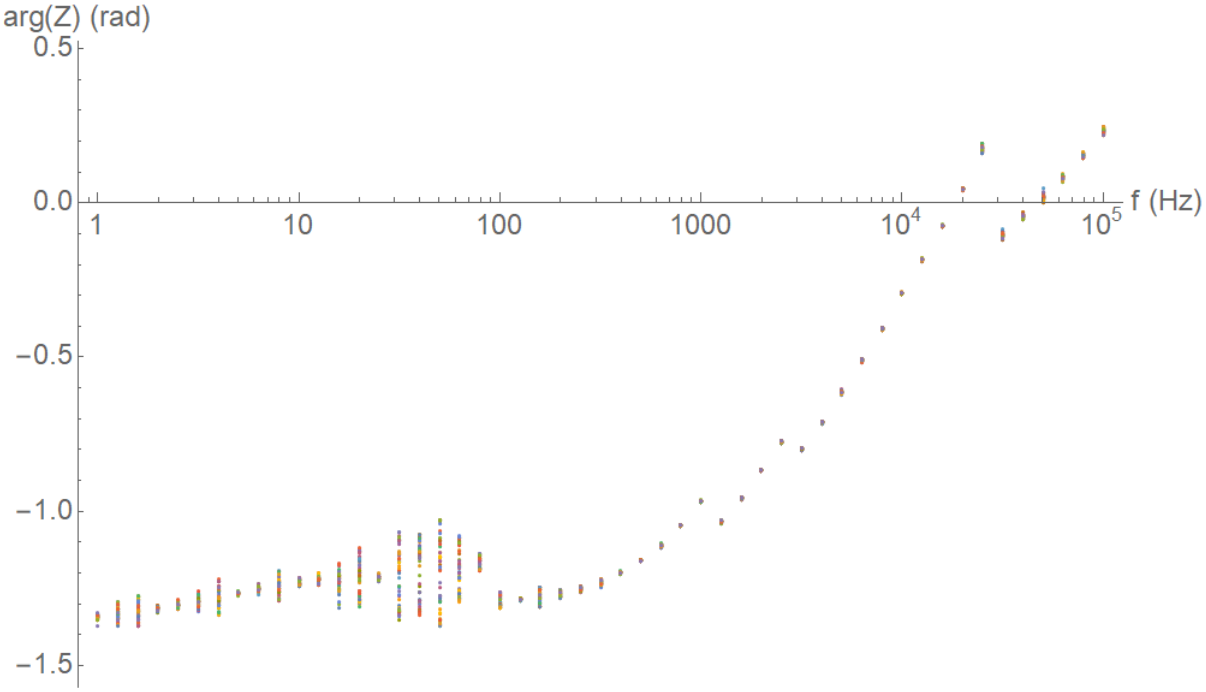

Figure 4.3: Impedance phase vs frequency, for 50 EIS measurements on a 0.1 M NaCl solution in the sensor compartment. Each colour represents a measurement. Noticeable is the low precision below 100 Hz, and a few discontinuities at higher frequencies.

In figure 4.3 we also see that the precision of the measurements is rather low below 100 Hz. Because of this, we decided to start measurements at a frequency of 100 Hz, instead of 1 Hz, in subsequent measurements.

In figure 4.8 we plotted the impedances in the complex plane. Again 50 measurements are shown, and for each spectrum we plotted the values of all frequencies simultaneously. In this figure, we again see distinct lines of the different measuring ranges. We also see a strange artefact at higher impedances. Measurements at the same frequency form circles,

while they should give approximately the same value. We have no explanation for these artefacts, but we cannot use these points in the data processing. This means that we will not use the data points with frequencies lower than 400 Hz.

4.3 Diffusion rate determination

The diffusion rate was determined when no potential is applied to the carbon membrane. For this the electrical impedance spectrum is measured every 10 seconds during almost 2 hours. The spectrum is measured with frequencies ranging from 100 Hz to 100 kHz. After 5 minutes the extra salt is added to the bulk compartment.

In figure 4.9 we see the impedances in the complex plane, for the 25 measurements before the salt is added. As these measurements all have the same salt concentration, the EIS measurements should be more or less the same. In the figure, we see that this is the case for the lower frequencies. The imprecision is quite a bit higher for the six highest frequencies (from 32 kHz to 100 kHz). We also see that these values are not in the same line as the other values. In section 4.2 we already saw that these six frequencies are in a measuring range that is not well calibrated with the other ranges. Therefore we will not use these points, and restrict to the frequencies from 400 Hz to 25 kHz (this corresponds to angular frequencies between $2.5 \times 10^3\,\mathrm{rad\,s^{-1}}$ and $1.6 \times 10^5\,\mathrm{rad\,s^{-1}}$).

We take a predictor of the form $\tilde{Z} = \frac{1}{1/R - i\omega C} + \frac{e^{-n\pi i/2}}{q_0 \omega^n}$, and we minimize $\sum_\omega \left| Z - \tilde{Z} \right|^2$ by varying R, C, n and q_0, where the sum ranges over all ω in the frequency range 400 Hz to 25 kHz. These give good fits, and allow us to extract the value of R from the spectrum. Typical values of the fitted parameters are $R = 3000\,\Omega, q_0 = 1.6 \times 10^{-7}, n = 0.86, C = -0.15\,\mathrm{nF}$. This produces a negative value for the capacitance, which is physically impossible. This means that we don't have a real physical basis for this model. Because it gives a relatively good fit, we nevertheless use it to find values of R.

We repeat this for all measured spectra, and this tells us how the resistance varies over time. Because concentration is inversely proportional to the resistance, we plot the conductance (the inverse of the resistance) against time. This is shown in figure 4.4 in blue dots.

After approximately 5 minutes, extra salt was added to the bulk compartment. In the plot, we see that from this moment the conductance increases, and after some time equilibrium is reached and the conductance is almost constant. However, it seems that we do not really yield a constant value.

This can be explained by the presence of the reference electrode in the system. Through the salt bridge of the reference electrode, a small amount of concentrated potassium chloride will leak into the bulk compartment. Concentrated potassium chloride is approximately 5 M, and the reference electrode leaks at about 10 µL per hour [14]. This yields 50 µmol KCl per hour. The bulk solution is about 20 mL, so the increase is in the order of 2.5 mM per hour. Since the added salt increased the NaCl concentration

in the bulk compartment by about 10 mM, the leaking of the reference electrode gives a noticeable linear background.

We want to find the time scale of the equilibration of the concentration. To do this, we fit the following formula to the data: $1/R = c_1 + c_2 t - c_3 e^{-t/\tau}$. Here c_1, c_2, c_3 are constants, and τ is the time scale of equilibration. We see in the figure that the data points in the first 11 minutes don't follow the same shape as the last part of the graph. Therefore we removed these points when fitting the formula. The resulting fit is shown in 4.4 as a yellow line. The value of τ obtained is 18.5 min. The values of the other constants are $c_1 = 355.2 \times 10^{-6}\,\Omega^{-1}, c_2 = 0.020 \times 10^{-6}\,\Omega^{-1}/\text{min}, c_3 = 48.6 \times 10^{-6}\,\Omega^{-1}$.

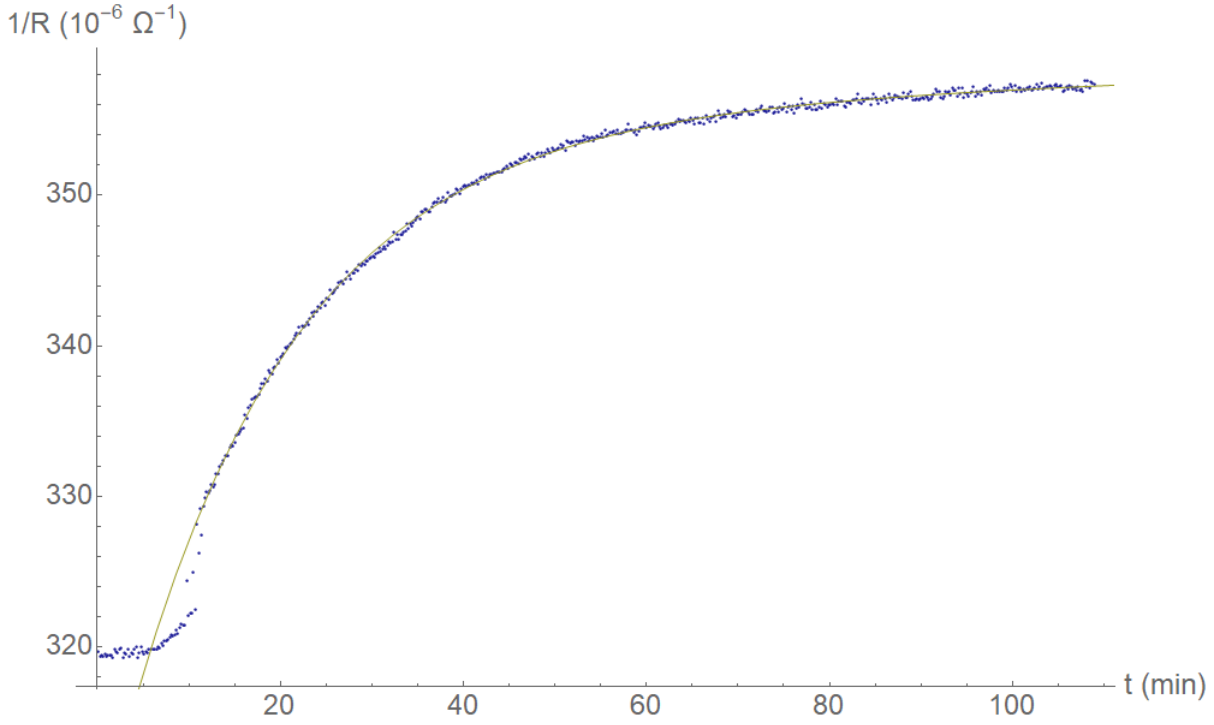

Figure 4.4: Conductance $(1/R)$ of solution in the sensor compartment, over time. Blue points are the values obtained from fitting the EIS data. The yellow line is fitted as exponential decay, with linear background.

4.4 EIS measurements while carbon membrane is electrified

The second research question was whether we could still measure the diffusion rate while the carbon was charged. During the charging of the carbon as described in section 4.1, we continuously did EIS measurements. At each potential, after the current had stabilised, we added salt to measure the diffusion.

In figure 4.10 we see the spectrum measured when the potential of the membrane was 330 mV, and when no salt was added. We see that this differs significantly from the spectrum in the above section. First of all, the values are much larger. And secondly

we see that there are values landing in the bottom-left quadrant. This means that the electrical circuit performs a negative amount of work. This is physically impossible, hence we have to conclude that the second potentiostat, which charges the carbon, influences the EIS measurements.

An explanation for this influence could be the following. The working of the potentiostat is such that the working electrode of both potentiostats are connected to the ground of the apparatus. This means that both working electrodes in the system are at the ground potential. The working electrodes in the setup are the carbon membrane and one of the platinum tips. They are both in contact with the same solution, but they have different double layers on their surface. Therefore the potential difference between each electrode and the solution is different. Because the apparatus sets both electrodes to the same (ground) potential, this must be compensated by an electric field in the solution, between the carbon membrane and one of the platinum tips. This electric field probably is a possible cause for the change of the electrical impedance spectrum, but this is not fully investigated. There may be other reasons for this drastic change.

We can find a workaround for this problem. For this we consider the equivalent circuit used to analyse the EIS measurements in section 4.3. This uses the impedance (we changed the sign of C)

$$Z = \frac{R}{1 - i\omega RC} + \frac{e^{-n\pi i/2}}{q_0 \omega^n}.$$

With the typical values $R = 3000\,\Omega, C = 0.15\,\mathrm{nF}, q_0 = 1.6 \times 10^{-7}, n = 0.86$, and ω at most $1.6 \times 10^5\,\mathrm{rad\,s^{-1}}$ we see that ωRC is at most 0.07. So the first term of the impedance is almost equal to R. On the other hand, we see that the second term has absolute value $\sim 45\,\Omega$ when $\omega = 1.6 \times 10^5\,\mathrm{rad\,s^{-1}}$. So for this value of ω, the impedance is approximately equal to R.

When examining the data, it seems that the following gives a good empirical fit to the spectrum:

$$Z = R - \frac{1}{q_1 \omega^2} + \frac{1}{q_0 (i\omega)^n}.$$

When ω becomes large, we again see that the impedance tends to the value R, so we assume that this value R is approximately the resistance of the solution. There is however no physical basis for this model, so we should be careful with drawing conclusions from these obtained resistances.

To choose the frequency range for the analysis, we again plot the phase of the impedance versus the frequency. This is shown in figure 4.5. As in section 4.2, we see that the frequencies above 25 kHz are in a very distinct measuring range. We also see a slight offset between 2 kHz and 2.5 kHz. Because we are mainly interested in the values obtained for high frequencies, we choose to use only frequencies from 2.5 kHz to 25 kHz.

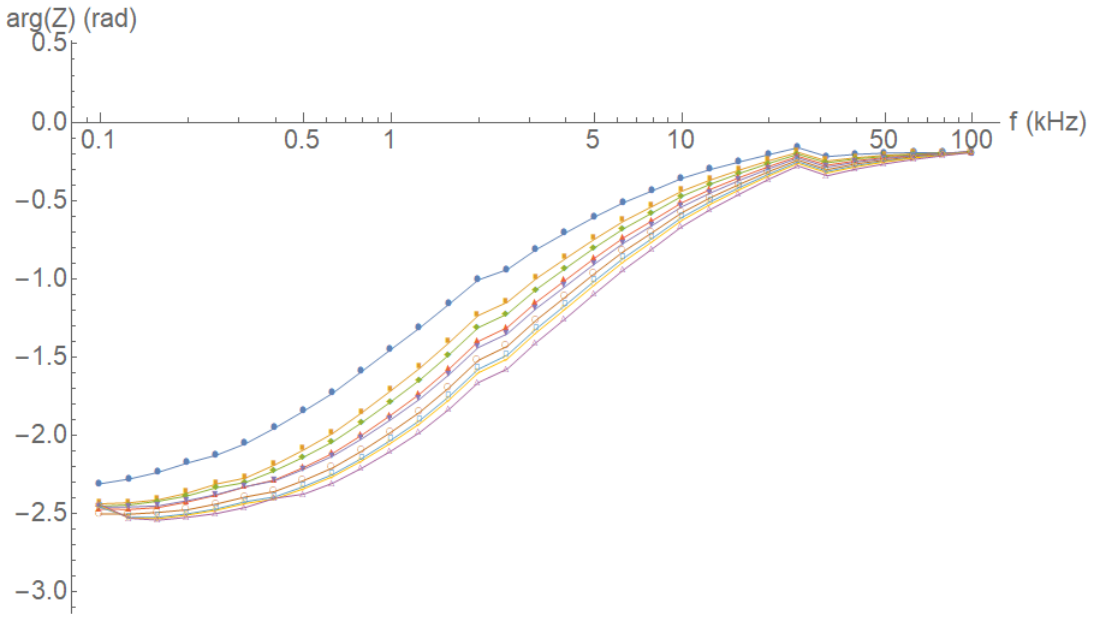

Figure 4.5: Impedance phase vs frequency, for 9 EIS measurements in the sensor compartment while the carbon membrane is electrified. Each colour represents a measurement. Noticeable are discontinuities around 2 kHz and 30 kHz.

4.5 Salt diffusion through electrified porous carbon

We have now chosen the data points to use, and the model to fit the data points to. The fitting is done in the same way as in 4.3. The resistances produced in this procedure are shown in figure 4.6. The red dots indicate when an extra amount of salt is added, and the green dots indicate when the potential of the carbon membrane is changed.

The general trend of the graph is clearly a linear increase of concentration over time. This is again caused by the leaking of the reference electrode. As pointed out in section 4.3, the leaking reference electrode causes a concentration increase of the order of 2.5 mM per hour, while the added extra salt gives an increase of 10 mM. Over the time scale of 80 hours, it is therefore to be expected that the leaking of the reference electrode will be dominant.

Even though the leaking of the reference electrode is dominant, we do see the effect of the added salt. After each red dot, the concentration will temporarily increase faster.

We also note that some artefacts are present in this figure. At each green dot, when the potential of the membrane is changed, we see a jump in the graph. And each time we see that there is again a jump some time later, which seems to return to the trend before the green dot. Because of this, we expect that these are artefacts caused by the electrical influence of the two electrometers on each other.

Apart from these jumps, there are also some jumps at other places: at $t = 0\,\text{h}, 1\,\text{h}, 34\,\text{h}, 71\,\text{h}$. These jumps can be caused by irregularities in the EIS measurement, although there is no apparent reason for these irregularities. Another reason can be errors in the fitting

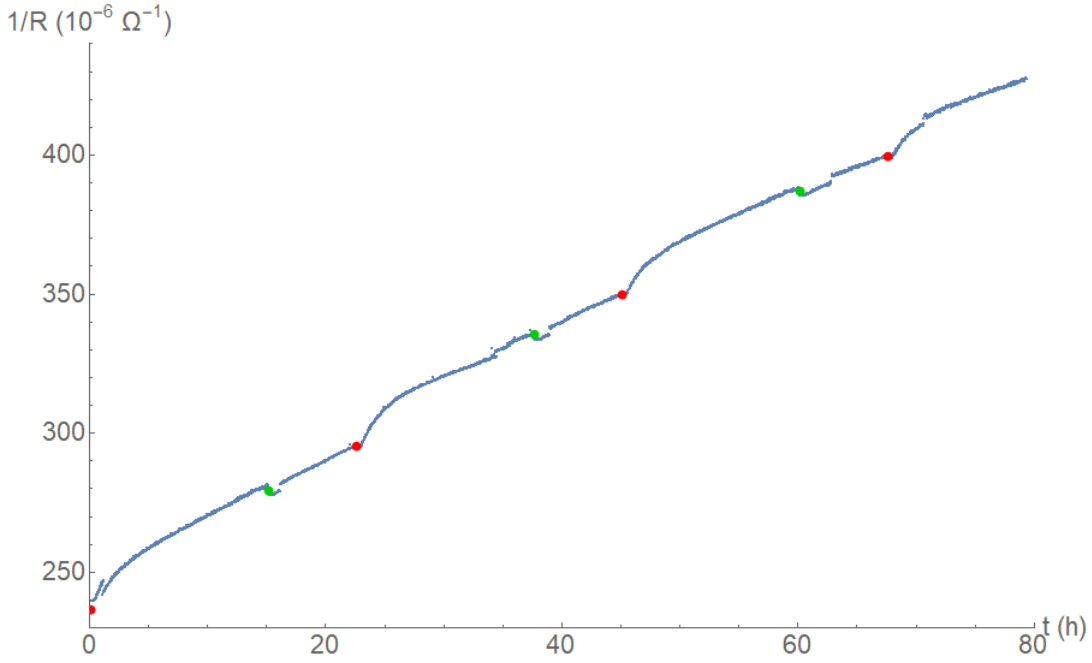

Figure 4.6: Conductance $(1/R)$ of solution in the sensor compartment, over time, while the carbon membrane is electrified. Blue points are the values obtained from fitting the EIS data. The green dots indicate when the potential of the carbon membrane is increased, the red dots indicate when extra salt is added to the bulk compartment.

procedure, because the artificial model is not entirely correct. We did not find out which of the two was the reason.

Just as in 4.3, we want to find the equilibration time of the concentration in the sensor compartment for all four instances where we increased the salt concentration. This means we want to fit the formula $1/R = c_1 + c_2 t - c_3 e^{-t/\tau}$ to the four parts of the plot. However this analysis is complicated by the presence of the jumps in the spectrum.

For the third salt addition, we can simply take the part of the data from the salt increase (red dot) until the membrane potential was changed (green dot), as there are no jumps in this part. For the second salt addition we can take the part from the salt addition until the jump around $t = 34\,\mathrm{h}$. However, for the first and fourth salt addition, there are jumps in the beginning and we cannot simply fit the formula to those parts of the graph.

To remedy this, we assume that the jumps move the plot up by a constant amount, so that we can subtract a constant value from all shifted data points to get them in line with the other data points. With this assumption, this shift value is really another fit parameter. Fitting the formula $1/R = c_1 + c_2 t - c_3 e^{-t/\tau}$, together with a shift of $-c_4$ for the parts of the plot that are 'jumped', we can also find the equilibration time for the first and fourth salt addition.

The values of the equilibration time are shown in table 4.7. First of all, we note that these values are quite a bit larger than the equilibration time when the carbon is not charged. In section 4.3 we saw that this equilibration time was 18.5 min, while the potential was about 330 mV in that case as well. So the two potentiostats do not only influence each

V vs Ag/AgCl (mV)	ΔQ (C)	τ (min)
330	0.00	89.0
430	0.17	104.3
530	0.36	100.4
630	0.61	98.3

Figure 4.7: Charge difference on the carbon, relative to the point $V_{WE-RE} = 330\,\mathrm{mV}$.

other, but they also influence the diffusion from the bulk compartment to the tips in the sensor compartment.

Furthermore, we also see that the equilibration times do not vary too much with the charge on the membrane. In section 2.1 we have seen that the macropores of the carbon membrane are much larger than the thickness of the double layer, while the micropores are of the same size. Because there is little effect of the surface charge on the salt diffusion rate, it must be the case that the salt mainly diffuses through the macropores. This is in line with the literature, where it is shown that the micropores are mainly responsible for storing the charge of the electric double layer [6]. To see more clearly the effect of charge on the membrane, we would need a carbon membrane with pores in the same range as the Debye length.

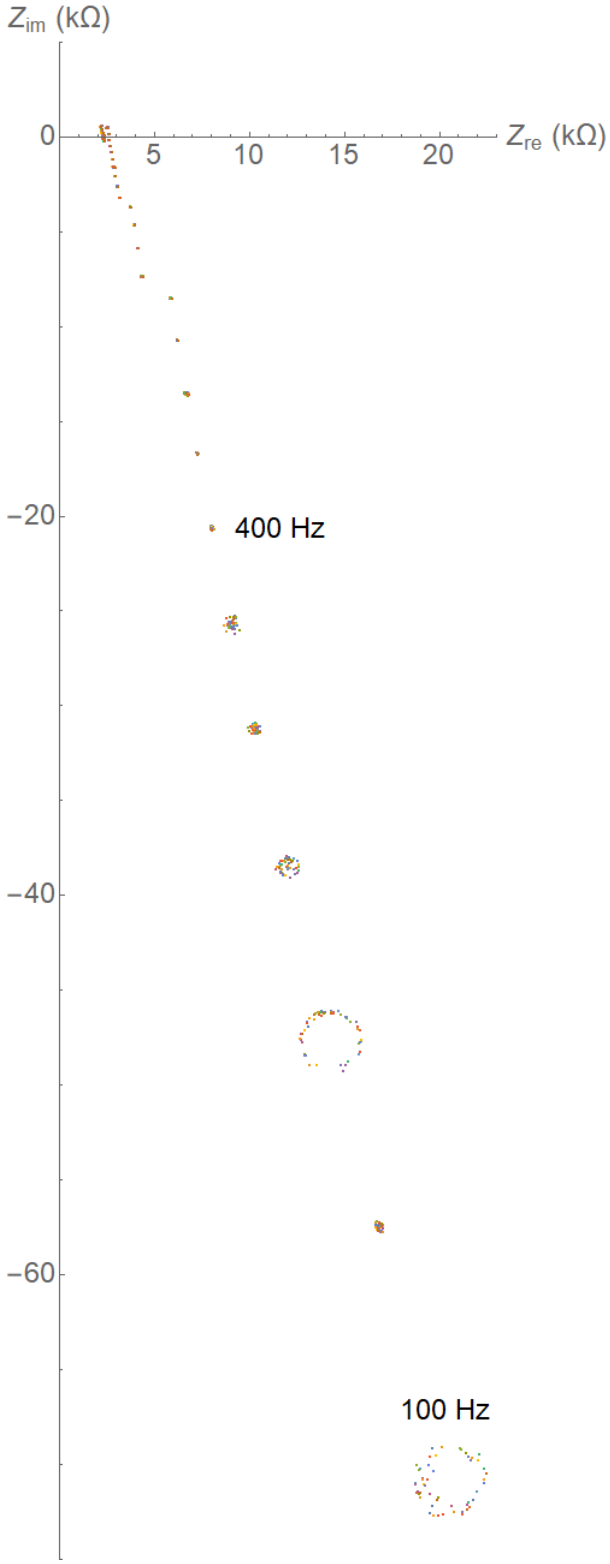

Figure 4.8: Impedance in the complex plane, for 50 EIS measurements on a 0.1 M NaCl solution in the sensor compartment. Each colour represents a measurement, for each measurement all frequencies are shown simultaneously.

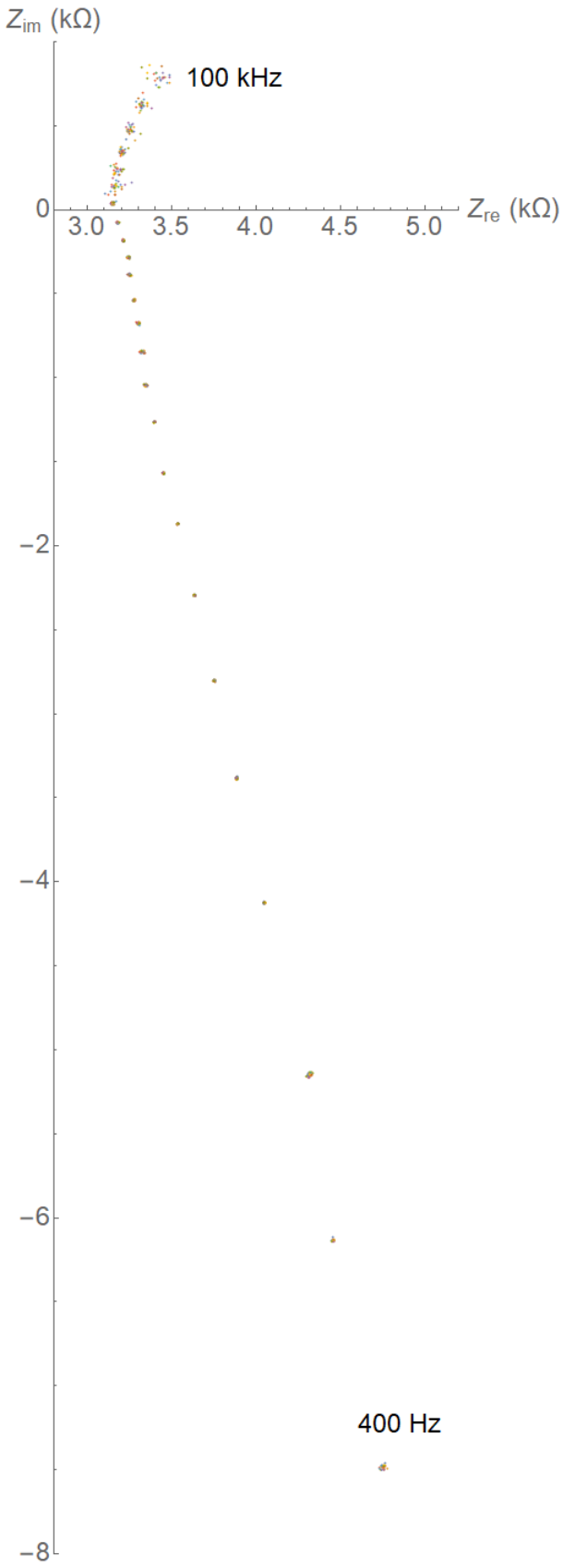

Figure 4.9: Impedance in the complex plane, for 25 EIS measurements in the sensor compartment, before extra salt is added. Each colour represents a measurement, for each measurement all frequencies are shown simultaneously.

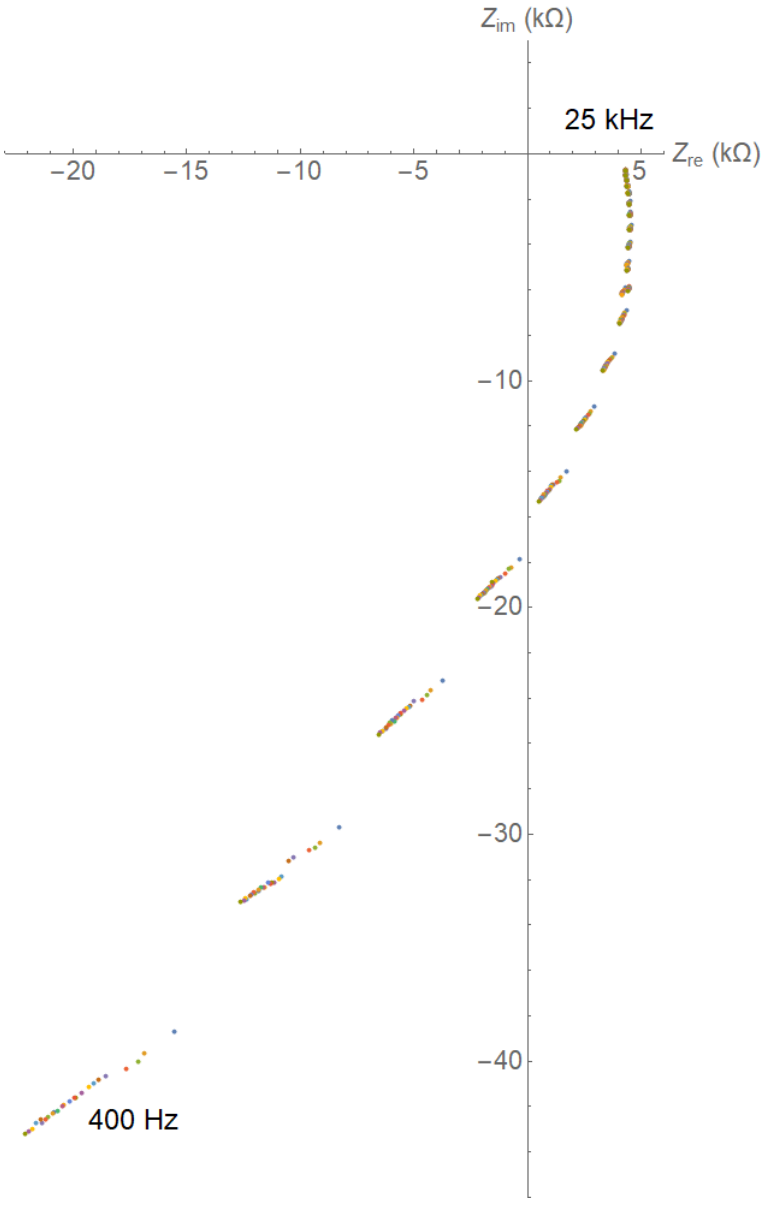

Figure 4.10: Impedance in the complex plane, for 25 EIS measurements in the sensor compartment, while the carbon membrane is electrified. Each colour represents a measurement, for each measurement all frequencies are shown simultaneously.

Chapter 5

Conclusion and outlook

We can now answer our research questions. First of all, we can indeed measure the diffusion rate of salt through porous carbon mounted as the membrane in the colloidal charge sensor. When we charge the carbon membrane, the EIS measurement to determine the solution resistance changes drastically. Despite this, we can still estimate the resistance and this allows us the measure the diffusion rate when the membrane is charged. We measured the diffusion rate at four different membrane potentials. The diffusion rate did not change too much, because transport across the membrane occurs mainly via macropores much wider than the thickness of the electric double layer. We could not exactly determine how the diffusion rate depends on the membrane charge, as we were only able to measure charge differences and not the point of zero charge.

5.1 Outlook

As indicated in the theory, we have not made theoretical predictions of the diffusion rate when the pore size is comparable to the double layer thickness. This could predict the outcome of the measurements on different carbon membranes.

We have also seen a number of issues in measuring the diffusion rate when the carbon membrane is charged. The reference electrode used leaks quite much, and this gives a larger effect than the manual additions of salt. Using a reference electrode that leaks less, or not at all, could give clearer results.

Charging the carbon membrane has a large influence on the EIS measurements, and we expected this is caused by the grounding in the measurement apparatus. Finding a way to 'decouple' the two measuring systems could give better EIS measurements.

In the EIS measurements we also encountered many instances where different measuring ranges were not well calibrated, or where there was a very large imprecision. This can likely be solved by doing a thorough calibration of the apparatus. Finding a way to prevent certain artefacts from occurring would also result in better data analysis.

The last research question could only be partially answered, as we could not determine the point of zero charge of the membrane. In the literature, methods have been described to determine this point [13], and this could help answer the third research question more fully.

As last point, we notice that the diffusion measurements generally have long equilibration times. When the carbon is charged they exceed 1.5 hours. These equilibration times could be decreased if the sensor compartment would be smaller. This requires investigation into new possible setups for these measurements.

Bibliography

[1] Albert P. Philipse, Bonny W. M. Kuipers, and Agienus Vrij. "A thermodynamic gauge for mobile counter-ions from colloids and nanoparticles". In: *Faraday Discuss.* 181 (2015), pp. 103–121. DOI: 10.1039/C4FD00261J. URL: http://dx.doi.org/10.1039/C4FD00261J.

[2] Jos van Rijssel et al. "Thermodynamic Charge-to-Mass Sensor for Colloids, Proteins, and Polyelectrolytes". In: *ACS Sensors* 1.11 (2016), pp. 1344–1350. DOI: 10.1021/acssensors.6b00510. URL: http://dx.doi.org/10.1021/acssensors.6b00510.

[3] Doriano Brogioli. "Extracting Renewable Energy from a Salinity Difference Using a Capacitor". In: *Phys. Rev. Lett.* 103 (5 July 2009), p. 058501. DOI: 10.1103/PhysRevLett.103.058501. URL: https://link.aps.org/doi/10.1103/PhysRevLett.103.058501.

[4] "3 - Electric Double Layers". In: *Solid-Liquid Interfaces*. Ed. by J. Lyklema. Vol. 2. Fundamentals of Interface and Colloid Science. Academic Press, 1995, pp. 1–232. DOI: https://doi.org/10.1016/S1874-5679(06)80006-1. URL: http://www.sciencedirect.com/science/article/pii/S1874567906800061.

[5] Andreas Härtel et al. "Fundamental measure theory for the electric double layer: implications for blue-energy harvesting and water desalination". In: *Journal of Physics: Condensed Matter* 27.19 (2015), p. 194129. URL: http://stacks.iop.org/0953-8984/27/i=19/a=194129.

[6] P. M. Biesheuvel et al. "Attractive forces in microporous carbon electrodes for capacitive deionization". In: *Journal of Solid State Electrochemistry* 18.5 (May 2014), pp. 1365–1376. ISSN: 1433-0768. DOI: 10.1007/s10008-014-2383-5. URL: https://doi.org/10.1007/s10008-014-2383-5.

[7] V. Romero, M.I. Vázquez, and J. Benavente. "Study of ionic and diffusive transport through a regenerated cellulose nanoporous membrane". In: *Journal of Membrane Science* 433 (2013), pp. 152–159. ISSN: 0376-7388. DOI: http://dx.doi.org/10.1016/j.memsci.2013.01.012. URL: http://www.sciencedirect.com/science/article/pii/S0376738813000355.

[8] Jos van Rijssel et al. *Computer simulations on charged polymers*. Tech. rep. Utrecht University, 2014.

[9] William M. Haynes, ed. *CRC handbook of chemistry and physics*. 97th ed. CRC Press, 2016. ISBN: 9781498754293.

[10] Elian Griffioen. "Calorimetry of the Charging of Porous Carbon Electrodes for Blue Energy". bachelor's thesis. Utrecht University, 2015.

[11] D. Brogioli, R. Zhao, and P. M. Biesheuvel. "A prototype cell for extracting energy from a water salinity difference by means of double layer expansion in nanoporous carbon electrodes". In: *Energy Environ. Sci.* 4 (3 2011), pp. 772–777. DOI: 10.1039/C0EE00524J. URL: http://dx.doi.org/10.1039/C0EE00524J.

[12] S. Porada et al. "Review on the science and technology of water desalination by capacitive deionization". In: *Progress in Materials Science* 58.8 (2013), pp. 1388–1442. ISSN: 0079-6425. DOI: http://dx.doi.org/10.1016/j.pmatsci.2013.03.005. URL: http://www.sciencedirect.com/science/article/pii/S0079642513000340.

[13] Tingting Wu et al. "Surface-treated carbon electrodes with modified potential of zero charge for capacitive deionization". In: *Water Research* 93 (2016), pp. 30–37. ISSN: 0043-1354. DOI: http://dx.doi.org/10.1016/j.watres.2016.02.004. URL: http://www.sciencedirect.com/science/article/pii/S0043135416300641.

[14] Mark Vis et al. "Donnan Potentials in Aqueous Phase-Separated Polymer Mixtures". In: *Langmuir* 30.20 (2014). PMID: 24787578, pp. 5755–5762. DOI: 10.1021/la501068e. URL: http://dx.doi.org/10.1021/la501068e.